

## Reducing modeling error of graphical methods for estimating volume of distribution measurements in PIB–PET study

Hongbin Guo<sup>a,\*</sup>, Rosemary A. Renaut<sup>a</sup>, Kewei Chen<sup>b</sup>, Eric M. Reiman<sup>b</sup>

<sup>a</sup>Arizona State University, School of Mathematical and Statistical Sciences, Tempe, AZ 85287-1804, United States

<sup>b</sup>Banner Alzheimer Institute and Banner Good Samaritan Positron Emission Tomography Center, Phoenix, AZ 85006, United States

### ARTICLE INFO

#### Article history:

Received 12 January 2010

Received in revised form 26 April 2010

Accepted 4 May 2010

Available online 20 May 2010

#### Keywords:

Bias

Modeling error

Graphical analysis

PET quantification

### ABSTRACT

Graphical analysis methods are widely used in positron emission tomography quantification because of their simplicity and model independence. But they may, particularly for reversible kinetics, lead to bias in the estimated parameters. The source of the bias is commonly attributed to noise in the data. Assuming a two-tissue compartmental model, we investigate the bias that originates from modeling error. This bias is an intrinsic property of the simplified linear models used for limited scan durations, and it is exaggerated by random noise and numerical quadrature error. Conditions are derived under which Logan's graphical method either over- or under-estimates the distribution volume in the noise-free case. The bias caused by modeling error is quantified analytically. The presented analysis shows that the bias of graphical methods is inversely proportional to the dissociation rate. Furthermore, visual examination of the linearity of the Logan plot is not sufficient for guaranteeing that equilibrium has been reached. A new model which retains the elegant properties of graphical analysis methods is presented, along with a numerical algorithm for its solution. We perform simulations with the fibrillar amyloid  $\beta$  radioligand [11C] benzothiazole-aniline using published data from the University of Pittsburgh and Rotterdam groups. The results show that the proposed method significantly reduces the bias due to modeling error. Moreover, the results for data acquired over a 70 min scan duration are at least as good as those obtained using existing methods for data acquired over a 90 min scan duration.

© 2010 Elsevier Inc. All rights reserved.

### 1. Introduction

Graphical analysis (GA) has been routinely used for quantification of positron emission tomography (PET) radioligand measurements. These techniques have been utilized with either input data acquired from plasma measurements or using the time activity curve from a reference brain region. They have been used for calculation of tracer uptake rates, absolute volumes of distribution  $V_T$  ( $\text{mL cm}^{-3}$ ) and distribution volume ratios (DVR), or, equivalently, for binding potentials ( $BP_{ND}$ ,  $BP_F$  and  $BP_P$ , all with the same units  $\text{mL cm}^{-3}$ ). They are widely used because of their inherent simplicity and general applicability regardless of the specific compartmental model.

The well-known bias, particularly for reversible kinetics, in parameters estimated by GA is commonly attributed to noise in the data [1–3], and therefore techniques to reduce the bias have concentrated on reducing the impact of the noise [4–7,2,8,9]. Here, we turn our attention to another important source of the bias: the modeling error which is implicit in GA approaches.

The bias associated with GA approaches has, we believe, three possible sources. The bias arising due to random noise is most often discussed, but errors may also be attributed to the use of numerical quadrature and an approximation of the underlying compartmental model. It is demonstrated in Section 2 that not only is bias an intrinsic property of the linear model for limited scan durations, which is exaggerated by noise, but also that it may be dominated by the effects of the modeling error. Indeed, numerical simulations, presented in Section 4, demonstrate that large bias can result even in the noise-free case. Conditions for over- or under-estimation of  $V_T$  due to modeling error and the extent of bias of the Logan plot are quantified analytically. These lead to the design of a bias correction method, Section 3, which still maintains the elegant simplicity of GA approaches. This bias reduction is achieved by the introduction of a simple non-linear term in the model. While this approach adds some moderate computational expense, simulations reported in Section 4.3 for the fibrillar amyloid  $\beta$  radioligand [11C] benzothiazole-aniline (Pittsburgh Compound-B [PIB]) [10], illustrate that it greatly reduces bias. Relevant observations are discussed in Section 5 and conclusions presented in Section 6. The necessary mathematical analyses are presented in the *Appendices*.

\* Corresponding author. Tel.: +1 480 965 8002; fax: +1 480 965 4160.  
E-mail address: [hobie.guo@gmail.com](mailto:hobie.guo@gmail.com) (H. Guo).

## 2. Theory

### 2.1. Existing linear methods

For the measurement of  $V_T$ , existing linear quantification methods for reversible radiotracers with a known input function, i.e. the unmetabolized tracer concentration in plasma, are based on the following linear approximation of the true kinetics [11]:

$$MA0 : \int_0^t C_T(\tau) d\tau \approx V_T \int_0^t C_p(\tau) d\tau - b C_T(t), \quad t \geq t_{eq}. \quad (1)$$

Here  $C_T(t)$  is the measured *tissue time activity curve* (TTAC),  $C_p(t)$  is the *input function*,  $V_T$  represents the *volume of distribution* and quantity  $b$  is a constant. This model, which we denote by MA0 to distinguish it from MA1 and MA2 introduced in [2], approximately describes tracer behavior at equilibrium i.e.  $t \geq t_{eq}$ . Dividing through by  $C_T(t)$ , showing that  $V_T$  is the linear slope and  $-b$  the intercept, yields the original Logan graphical analysis model, denoted here by Logan-GA,

$$Logan-GA : \frac{\int_0^t C_T(\tau) d\tau}{C_T(t)} \approx V_T \frac{\int_0^t C_p(\tau) d\tau}{C_T(t)} - b, \quad t \geq t_{eq}. \quad (2)$$

With known  $C_T(t)$  and  $C_p(t)$ ,  $V_T$  and intercept  $-b$  are obtained by using linear least squares (LS) for the sampled version of (2). Although it is well-known that this model often leads to under-estimation of  $V_T$  it is still widely used in PET studies. An alternative formulation based on (1) is the MA1,

$$MA1 : C_T(t) \approx \frac{V_T}{b} \int_0^t C_p(\tau) d\tau - \frac{1}{b} \int_0^t C_T(\tau) d\tau, \quad t \geq t_{eq}, \quad (3)$$

for which  $V_T$  can again be obtained using LS [2]. The focus here is thus examination of the modeling error specifically for Logan-GA and MA1, from which a new method for reduction of modeling error is designed.

### 2.2. Modeling error analysis

The general three-tissue compartmental model for the reversible radioligand binding kinetics of a given brain region or a voxel is illustrated in Fig. 1 [12,13]:

Here  $C_p(t)$  (kBq mL<sup>-1</sup>) is the input function, i.e. the unmetabolized radiotracer concentration in plasma, and  $C_{FT}(t)$ ,  $C_{NS}(t)$  and  $C_S(t)$  (kBq mL<sup>-1</sup>) are free radioactivity, non-specific bound and specific bound tracer concentrations, resp., and  $K_1$  (mL mL<sup>-1</sup> min<sup>-1</sup>) and  $k_i$  (min<sup>-1</sup>),  $i = 2, \dots, 6$ , are rate constants.  $V_T$  is related to the rate constants as follows [14]:

$$V_T = \frac{K_1}{k_2} \left( 1 + \frac{k_3}{k_4} + \frac{k_5}{k_6} \right). \quad (4)$$

The numerical implementation for estimating the unknown rate constants of the differential system illustrated in Fig. 1 is difficult because three exponentials are involved in the solution of this system [13,15]. Fortunately, for most tracers it can safely be assumed that  $C_{NS}$  and  $C_{FT}$  reach equilibrium rapidly for specific binding

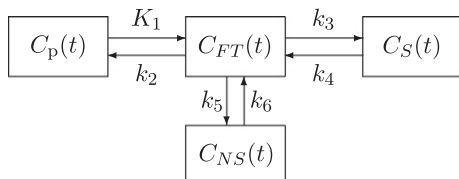


Fig. 1. Three-tissue compartmental model of reversible radioligand binding dynamics.

regions. Then it is appropriate to use a two-tissue four-parameter (2T-4k) model by binning  $C_{NS}(t)$  and  $C_{FT}(t)$  to one compartment  $C_{ND}(t) = C_{FT}(t) + C_{NS}(t)$ . This is equivalent to taking  $k_5 = k_6 = 0$ , and hence  $C_{NS}(t) = 0$ . On the other hand, for regions without specific binding activity, we know  $C_S(t) = 0$  which is equivalent to taking  $k_3 = k_4 = 0$ . For some tracers, however, for example the modeling of PIB in the cerebellar reference region, the best data fitting is obtained by using the 2T-4k model without binning  $C_{NS}(t)$  and  $C_{FT}(t)$  [16]. The advantage of using a 2T-4k model is that this model is *a priori* structurally globally (uniquely) identifiable [15,14]. Assuming the latter,  $V_T$  is given by  $K_1/k_2(1 + k_3/k_4)$ , and  $K_1/k_2(1 + k_5/k_6)$ , for regions with and without specific binding activity, resp. Ignoring the notational differences between the two models, for regions with and without specific binding activity, they are both described by the same abstract mathematical 2T-4k model equations. Here, without loss of generality, we present the 2T-4k model equations for specific binding regions,

$$\frac{dC_{ND}(t)}{dt} = K_1 C_p(t) - (k_2 + k_3) C_{ND}(t) + k_4 C_S(t) \quad (5)$$

$$\frac{dC_S(t)}{dt} = k_3 C_{ND}(t) - k_4 C_S(t). \quad (6)$$

To obtain the equations appropriate for regions without specific binding activity,  $C_S(t)$  is replaced by  $C_{NS}(t)$  and  $k_3$  and  $k_4$  are interpreted as the association and dissociation parameters of regions without specific binding activity. To simplify the explanation  $C_S(t)$ ,  $k_3$  and  $k_4$  are used throughout for both regions with and without specific binding activity, with the assumption that  $C_S(t)$ ,  $k_3$  and  $k_4$  should automatically be replaced by  $C_{NS}(t)$ ,  $k_5$  and  $k_6$  respectively, when relevant.

The solution of the linear differential system (5) and (6) is given by

$$C_{ND}(t) = (a_1 e^{-\alpha_1 t} + b_1 e^{-\alpha_2 t}) \otimes C_p(t) \quad (7)$$

$$C_S(t) = a_2 (e^{-\alpha_1 t} - e^{-\alpha_2 t}) \otimes C_p(t) \quad (8)$$

where  $\otimes$  represents the convolution operation,

$$\alpha_{1,2} = (k_2 + k_3 + k_4 \mp \sqrt{(k_2 + k_3 + k_4)^2 - 4k_2 k_4})/2, \quad \text{and} \\ a_1 = \frac{K_1(k_4 - \alpha_1)}{\alpha_2 - \alpha_1}, \quad b_1 = \frac{K_1(\alpha_2 - k_4)}{\alpha_2 - \alpha_1}, \quad \text{and} \quad a_2 = \frac{K_1 k_3}{\alpha_2 - \alpha_1}. \quad (9)$$

The overall concentration of radioactivity is

$$C_T(t) = C_{ND}(t) + C_S(t) \\ = ((a_1 + a_2) e^{-\alpha_1 t} + (b_1 - a_2) e^{-\alpha_2 t}) \otimes C_p(t). \quad (10)$$

Integrating (5) and (6) and rearranging, details are presented in Appendix A, yields

$$\int_0^t C_T(\tau) d\tau = V_T \int_0^t C_p(\tau) d\tau - \frac{k_3 + k_4}{k_2 k_4} C_{ND}(t) - \frac{k_2 + k_3 + k_4}{k_2 k_4} C_S(t), \quad (11)$$

$$= V_T \int_0^t C_p(\tau) d\tau - \frac{k_3 + k_4}{k_2 k_4} C_T(t) - \frac{1}{k_4} C_S(t). \quad (12)$$

This is model (1) when  $C_S(t)$  is linearly proportional to  $C_T(t)$  for a time window within the total scan duration of  $T$  minutes. The accuracy of linear methods based on (1) is thus dependent on the validity of the assumption that  $C_S(t)$ , or equivalently  $C_{ND}(t)$ , is approximately linearly proportional to  $C_T(t)$  over a time window within  $[0, T]$ . Logan observed that  $C_{ND}(t)$  and  $C_S(t)$  are roughly proportional to  $C_T(t)$ , after some time point  $t^*$  ( $< t_{eq}$ ) [11]. If the assumption of linear proportionality breaks down for the given window,  $[t^*, T]$ , modeling error will be introduced in the estimated  $V_T$ , as shown later in Section 4.3. Indeed, in Section 5.1 we show that, for the PIB radioligand on some regions with small  $k_4$ , there is no window within a 90 min scan duration where  $C_S(t)$  and  $C_T(t)$  are linearly proportional. This is despite the apparent good

Download English Version:

<https://daneshyari.com/en/article/4500643>

Download Persian Version:

<https://daneshyari.com/article/4500643>

[Daneshyari.com](https://daneshyari.com)